

The Significance of the Rouse Segment: Its Concentration Dependence

Tadashi Inoue,* Takehiko Uematsu, and Kunihiro Osaki

Institute for Chemical Research, Kyoto University, Kyoto 611-0011, Japan

Received June 18, 2001; Revised Manuscript Received October 25, 2001

ABSTRACT: Dynamic birefringence and dynamic viscoelasticity of polystyrene/tricresyl phosphate solutions were measured over a wide reduced frequency region from the rubbery to the glassy zone for concentrations ranging from 0.20 g cm⁻³ to bulk. The rubbery (polymeric) component of the modulus whose molecular origin is attributed to the segment orientation was separated from solvent contribution with aid of the modified stress–optical rule. The size of the Rouse segment was calculated from the limiting modulus of the rubbery component at high frequencies. The stress–optical coefficient, which is a measure of size of the optical segment, was found to be insensitive to polymer concentration. This result indicates that the main chain orientation created by the unit stress is insensitive to polymer concentration, implying that statistical nature of polymer chain is not affected by the presence of solvent. This result is in accord with a conformational study, which indicates that the radius of gyration of PS chains is almost constant at any concentration. On the other hand, with decreasing concentration, the estimated molecular weight of the Rouse segment increased from 900 for bulk to the reported value of 5000 for dilute solutions. It is shown that the Rouse segment can be related to the instantaneous main chain orientation induced by unit deformation. The larger value of the Rouse segment size in dilute solution indicates that the strain-induced main chain orientation (orientation of backbone) in solution is reduced compared with that in bulk. The molecular origin of the present results may be attributed to the difference of the rigidity between the solvent and the polymer chain in the glassy region, which would cause inhomogeneous strain distribution in local scale and suppress the main chain orientation.

Introduction

When a polymeric material is deformed, it becomes anisotropic and birefringent. The birefringence has a strong relationship with the stress. For the case of polymer melts or concentrated solutions, the stress–optical rule, SOR, holds valid between deviatoric parts of stress tensor, $\sigma(t)$, and the refractive index tensor, $\Delta n(t)$.¹

$$\Delta n(t) = C\sigma(t) \quad (1)$$

Here, C is the stress–optical coefficient. The validity of the SOR has been confirmed for many polymeric materials except low molecular weight polymer systems^{2,3} or solutions where solvent contribution cannot be ignored. The most significant indication of the rule is that the stress and birefringence have the same molecular origin: orientation of main chain.

The SOR does not hold in the glass-to-rubber transition zone or the glassy zone. The relationship between the stress and the birefringence for polymer melts may be described with the modified stress–optical rule, MSOR.⁴ The MSOR says that another component contributes to both the stress and birefringence in addition to the main chain orientation and that proportionality similar to the ordinary stress–optical rule holds well for the second component. The rule for tensile deformation can be written as follows:

$$E^* = E_R^* + E_G^* \quad (2)$$

$$O^* = C_R E_R^* + C_G E_G^* \quad (3)$$

Here $E^* \equiv E'(\omega) + iE''(\omega)$ is the complex Young's modulus, and $O^* \equiv O'(\omega) + iO''(\omega)$ is the complex strain–optical coefficient, which is the complex ratio of tensile birefringence to the strain. The suffices R and G respectively represent the rubbery and glassy components. C_i is the stress–optical coefficient for component i .

The R component is related to the main chain orientation because C_R is identical to C in the ordinary SOR. The other component, G, is the source of glassy features such as a high modulus and is interpreted to be related to twisting or rotation of structure units.⁵ The utility of the MSOR is that the main chain orientation in the glassy zone can be estimated from the combination of the stress and birefringence measurements.

The frequency dependence of E_R^* around the glass transition zone can be well described with the Rouse–Mooney model.⁶ This means that the relaxation of the main chain orientation in short time region can be described with the bead–spring theory. The limiting modulus of the R component at high frequencies, $E_R'(\infty)$, can be related to the Rouse segment.

$$M_S = \frac{3cRT}{E_R'(\infty)} \quad (4)$$

Here, c is polymer concentration and R is gas constant. T is temperature. The presence of the entanglement may affect height of $E_R'(\infty)$. However, its effect is estimated less than 5% for the case of PS, and therefore it may be ignored. For many polymer melts, thus determined M_S agrees with the Kuhn segment size determined as a geometrical parameter.⁷ For the case of PS melt, the value of M_S estimated in melts is approximately 900. This value is consistent with molecular weight of Kuhn segment size, M_K , of PS.

On the other hand, it is already known that the Rouse segment size of PS in dilute solution is fairly large: $M_S \sim 5000$.^{8–10} For the case of dilute solutions, complex viscosity was preferably provided. According to these studies, the complex shear viscosity, η^* , and a corresponding optical quantity, the mechanooptic ratio, $S^*(\omega)$, which is the ratio of birefringence to rate of shear, can be represented as a sum of two contributions. The first one is the polymer contribution, and the other one comes from solvent¹⁰

$$\eta^*(\omega) = \eta_{\text{poly}}^*(\omega) + \eta_{\infty} \quad (5)$$

$$S^*(\omega) = S_{\text{poly}}^*(\omega) + S_{\infty} \quad (6)$$

The second terms, η_{∞} and S_{∞} , represent *effective* solvent contribution, and therefore they are not identical to the value for neat solvent. η_{∞} and S_{∞} were frequency-independent constants and have been regarded as fitting parameters. In later studies, η_{∞} and S_{∞} were considered as a sum of more complex contributions.^{11,12} Usually, measurements on dilute solutions were performed with a glass-forming solvent, Aroclor. For a glass-forming solution, the effective solvent contributions, η_{∞} and S_{∞} , are frequency-dependent and therefore should be regarded as the complex quantities, particularly around its glass transition temperature. An example of the complex shear modulus of a dilute polystyrene solution in a glass-forming solvent can be found in a paper by Riande et al.¹³ Phenomenologically, eqs 5 and 6 can be written in a more generalized form as follows.

$$\eta^*(\omega) = \eta_{\text{poly}}^*(\omega) + \eta_{\infty}^*(\omega) \quad (7)$$

$$S^*(\omega) = S_{\text{poly}}^*(\omega) + S_{\infty}^*(\omega) \quad (8)$$

Equations 5 and 6 correspond to ignoring the elastic contributions of solvents.

Equations 5 and 6 have been used to estimate the main chain orientation term, η_{poly}^* and S_{poly}^* . In this context, eqs 5 and 6 provide an equivalent method to the MSOR. The polymer contributions, η_{poly}^* and S_{poly}^* , in dilute solutions can be well described with the beads-spring model, BSM, including the hydrodynamic interaction and excluded-volume effect. By fitting polymeric terms with BSM, M_S can be estimated. The estimated values of PS for dilute solutions are about 5000. This value is surprisingly large. Taken literally, this suggests that no conformational relaxations take place on a shorter scale. However, the characteristic ratio for PS implies a persistence length closer to 10 monomer units, clearly indicating that motions on a shorter scale must occur. Nevertheless, the estimated high value seems quite reasonable at least for Rouse properties. Amelar et al. measured S^* of low molecular weight polystyrenes and found that S_{poly}^* of PS solutions with $M = 5000$ can be well fitted with a single Rouse mode.¹⁰

On the contrary, the complex modulus for bulk polystyrene with about the same molecular weight shows seven Rouse modes in melts,¹⁴ indicating that M_S is much smaller than 5000, and therefore $M_S = 900$ for PS melts also looks reliable. Thus, there is large difference between the sizes of Rouse segment in melts and in solutions. In this study, we report the result of dynamic birefringence measurement on polystyrene solutions covering the moderate concentration regime to investigate the concentration dependence of the Rouse segment. We will consider the significance of the Rouse segment from the concentration dependence.

Another measure of the segment size is the stress optical coefficient, C . This quantity represents the orientational birefringence for unit stress. According to the molecular theory for strain-induced birefringence for rubbery materials, C can be related with the anisotropy of polarizability of the statistical segments.¹⁵ Calculations using the rotational isomeric model showed that anisotropy of polarizability of the segments is propor-

Table 1. Test Solutions

sample code	$M_w/10^6$	M_w/M_n	$c/\text{g cm}^{-3}$
f850/20	8.24	1.17	0.20
f850/30	8.24	1.17	0.30
f550/45	5.48	1.10	0.46
f288/60	2.89	1.09	0.62

tional to the number of repeating units per the segment.¹⁶ The concentration dependence of C over a wide concentration range is also our interest.

Experimental Section

The test solutions are described in Table 1. Polystyrene samples with sharp molecular weight distributions were purchased from Toso Co., Ltd. The solvent, tricresyl phosphate ($T_g = -68$ °C), was purchased from Wako Co. and was used without further treatment. The solutions were prepared following the literature.¹³ The glass transition temperature, T_g , of PS/TCP solutions was studied by Riande et al. The rheo-optical measurements were performed at $T \geq T_g$.

The samples were molded into a sheet at 50 °C and allowed to come to equilibrium for at least a month prior to use. The obtained sheet with 1 mm thickness was something like a soft rubber or gel. A 5 mm × 20 mm specimen was cut and attached to the fixture of the tensile tester as with ordinary solid film samples. We tried to extend the measurement to lower concentrations (0.1 g/cm³). However, the measurements were very difficult because the relaxation time of the sample was too short and the modulus was low.

The apparatus for dynamic birefringence measurements was reported elsewhere.⁴ The optical train for birefringence measurements was attached to a conventional tensile-type dynamic rheometer. The optical train was composed of a He-Ne laser ($\lambda = 632.8$ nm), a $\lambda/4$ plate, and two Glan-Taylor prisms. The frequency range of tensile strain was 1–130 Hz. The consistency of the mechanical data was checked with a standard shear rheometer, ARES, Rheometric Scientific, with parallel-plates fixture having 7.9 mm diameter.

Results

Composite Curves for Modulus and Birefringence. Figure 1 displays an example of the composite curves for the complex Young's modulus and the complex strain-optical coefficient. Here, the method of reduced variables was used:¹⁷ E' and E'' at different temperatures were plotted against frequency in a double-logarithmic scale and are shifted along the abscissa with a shift factor, a_T , so as to form smooth curves. Here we did not use any vertical shift for E^* . Although the data in the rubbery zone are limited, the composite curves cover a wide frequency region from a part of the rubbery zone to the glassy zone. The same method was used for O' and O'' , and the resulting shift

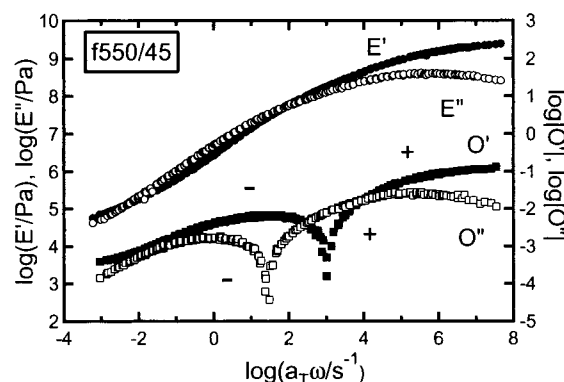


Figure 1. Complex Young's modulus and complex strain-optical coefficient for f550/45. $T_r = 10$ °C.

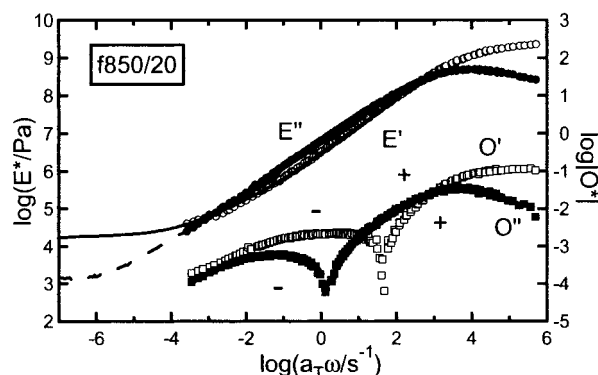


Figure 2. Complex Young's modulus and complex strain-optical coefficient for f850/20 solution. $T_r = -40$ °C. Lines represent complex shear modulus ($3G'$ and $3G''$) measured by a parallel-plate apparatus.

factor was slightly different from that for E^* . We did not use any vertical shift for O^* . Superposition for both E^* and O^* works quite well. However, the frequency span of the composite curves is slightly different, which indicates that the two have different temperature dependence.⁴ Similar results are obtained for many polymeric systems in melt.¹⁸ For the case of polymer solutions, Riande et al. measured the viscosity and the recoverable compliance around the glass transition zone of PS/TCP solutions over a wide concentration range covering 0–100 wt %. They reported that the viscosity and the recoverable compliance showed a different temperature dependence, except neat TCP. It was also reported that the polymer term and local term in eqs 5 and 6 showed a different temperature dependence. These results indicate that global motions of polymer chains controlling the viscosity show weaker temperature dependence than the local motions determining the viscoelasticity around the glass transition zone. We will come back to this issue later.

Characteristic features of O^* and E^* are almost the same as those for neat polystyrenes: The signs of O' and O'' are positive in the glassy zone and negative in the rubbery zone. The difference may be found in the broad shape of E'' around its maximum, which is a known effect of solvent for plasticized systems.¹⁷

Figure 2 illustrates composite curves for the lowest PS concentration sample, f850/20. Also included is the shear modulus measured with the shear rheometer. Compared with Figure 1, the shape of E'' around the E'' maximum is not so broad. This result may be natural because E'' should be reduced to that of neat TCP with decreasing polymer concentration. Another notable point is that negative part of O^* for f850/20 solution is lower compared with f550/45. Negative birefringence for PS is originated by the oriented segments, and therefore it would be natural to decrease with decreasing polymer concentration.

We calculated the tensile viscosity, η_E^* ($\equiv E^*/\omega$), and tensile mechanooptic ratio, S_E^* ($\equiv O^*/\omega$), from E^* and O^* data so that our result can be compared with studies for dilute solutions. Figure 3 illustrates η_E^* and S_E^* for f288/20. The frequency region of the composite curves obtained by traditional shear complex viscosity measurements for dilute solutions is limited to low frequencies, $\log(\omega a_T/s^{-1}) < 1$. In dilute solutions, the contribution of local motions has been regarded to be constant independent of frequency as eqs 4 and 5. If this is the case, a frequency-independent region should be observed

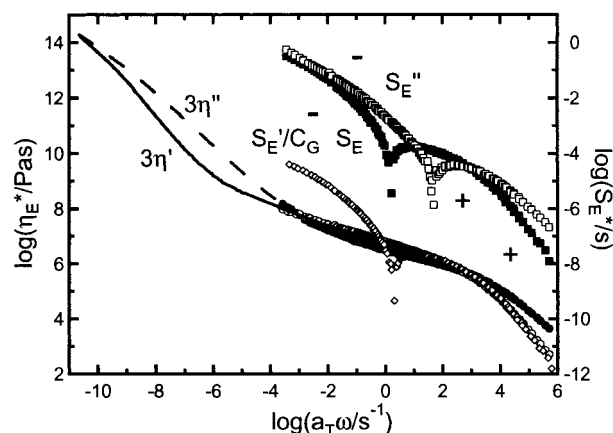


Figure 3. Complex viscosity and complex strain-optical coefficient for f850/20 solution. $T_r = -40$ °C. Lines represent complex shear viscosity ($3\eta'$ and $3\eta''$) measured by a parallel-plate apparatus.

for η_E' or S_E' at high frequencies. For the case of the present results, any frequency region was not observed where η' or S' is independent of ω . This is due to the glass transition of solution. Thus, eqs 5 and 6 did not work for the present case, and therefore we used eqs 7 and 8. If proportionality holds well between η_∞^* and S_∞^* , eqs 7 and 8 are reduced to the MSOR. In the following section we examine the applicability of the MSOR to the present data.

Stress-Optical Coefficients for MSOR. C_R of the MSOR is the stress-optical coefficient in the rubbery zone, and therefore it can be easily determined. On the other hand, C_G is defined as O'/E' at $\omega \rightarrow \infty$.⁴ For the case of polymer solutions, the glass forming solvent would contribute to the modulus around the glass transition zone. For such a case, O'/E' may depend on ω because solvent contribution may be different from polymer contribution. On the other hand, we may anticipate that solvent dynamics and polymer dynamics are cooperative and that optical contribution may be similar because both the solvent and polymer have a large optically anisotropic group, benzene ring. Consequently, O'/E' may be regarded as a constant over a wide frequency region; the MSOR could be a good first approximation.

Figure 4 shows a comparison of O' and E' for f550/45 at low temperatures. Here, the same shift factor was used for both O' and E' in order to compare them measured at the same temperature. O'/E' can be regarded to be independent of frequency and temperature, indicating the solution data can be analyzed with the ordinary MSOR. The obtained C_G value is 6.5×10^{-11} Pa⁻¹. This value is about 2 times larger than that for polystyrene in melt.⁴ With decreasing concentration, the frequency region where proportionality between O' and E' holds valid becomes narrow.

For the case of complex viscosity, $\eta_E^*(\omega) = \eta_E'(\omega) - i\eta_E''(\omega)$, and the tensile mechanooptic ratio, $S_E^*(\omega) = S_E'(\omega) - iS_E''(\omega)$, the MSOR can be written as follows:

$$\eta_E^*(\omega) = \eta_{ER}^*(\omega) + \eta_{EG}^*(\omega) \quad (9)$$

$$S_E^*(\omega) = C_R \eta_{ER}^*(\omega) + C_G \eta_{EG}^*(\omega) \quad (10)$$

C_G is defined as $S_E'(\omega)/\eta_E'(\omega)$ at $\omega \rightarrow \infty$. In Figure 3, $S_E'(\omega)/C_G$ is shown to check validity of the MSOR. Over

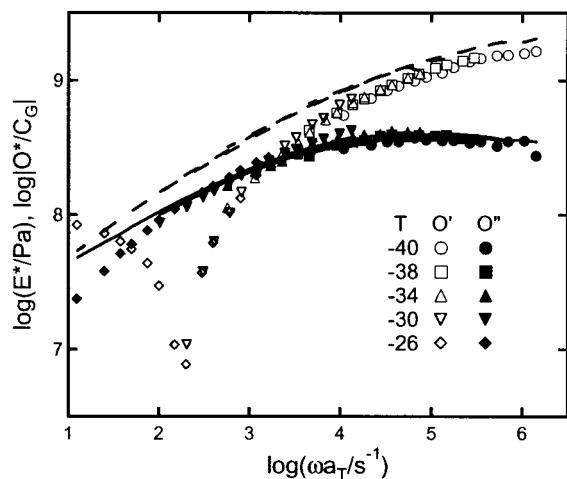


Figure 4. Frequency dependence of E^* and O^* for f550/45 at various temperatures. $T_r = -20$ °C. Dashed line, E' ; continuous line, E'' .

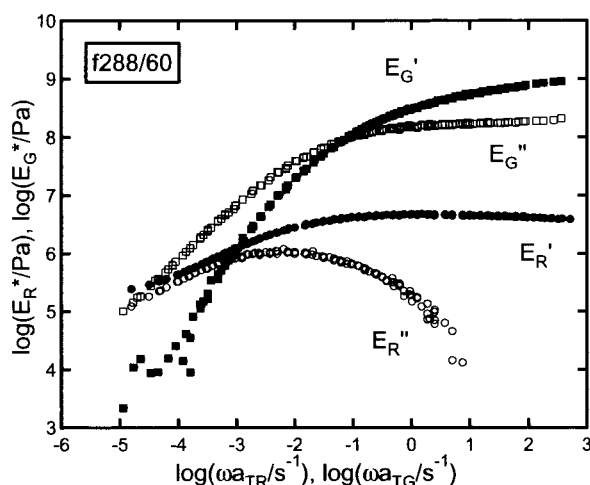


Figure 5. Component functions for f288/60 solution. $T_r = 10$ °C.

a wide range of high frequency, proportionality between $S_E'(\omega)$ and $\eta_E'(\omega)$ holds valid.

We do not intend to stress that the MSOR is generally valid for polymeric solutions including dilute solutions. However, we should note that for the moderate concentration regime the solvent contribution, which would be modified by the presence of polymer chain from that for the neat solvent, cannot be described with single constant value as eqs 5 and 6. For such a case, the solvent contribution should be represented with a frequency-dependent function. The present result shows that the MSOR provides a reasonable first-approximation function. Cooperative motions of polymers and solvent molecules may help to extend the applicable range of the MSOR. Thus, in the present analysis, the solvent contribution is included in the G component.

Separation into Component Functions. The MSOR equations, eqs 2 and 3, were solved for $E_R^*(\omega)$ and $E_G^*(\omega)$ with C_R and C_G determined with the method described above. Here, temperature dependence of C_R , which is theoretically expected to be $\sim 1/T$, was ignored because temperature range is narrow (see Figure 9). This procedure was performed for each simultaneously measured data set of $E^*(\omega)$ and $O^*(\omega)$. In the present study, we needed to determine geometrical factors for the gellike samples. This procedure was less accurate

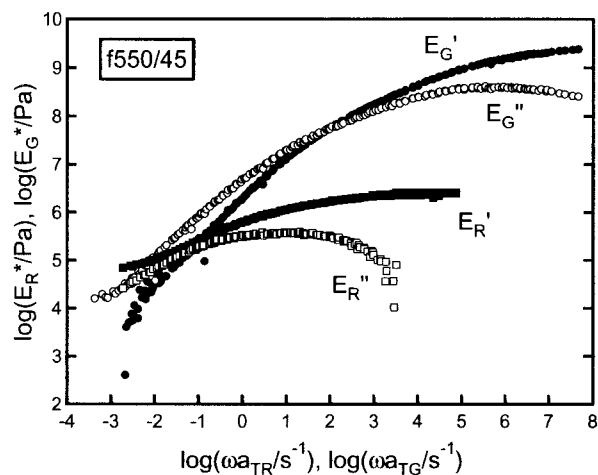


Figure 6. Component functions for f550/45 solution. $T_r = -20$ °C.

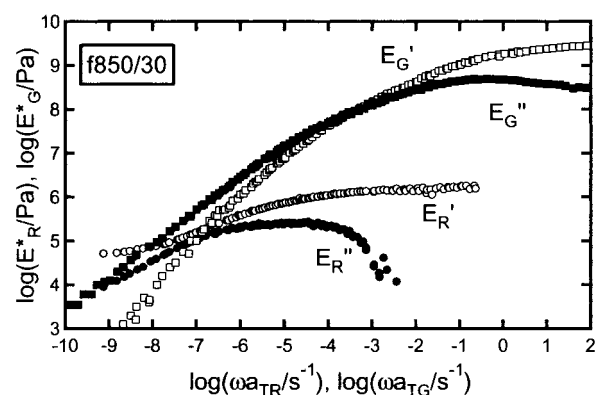


Figure 7. Component functions for f288/30 solution. $T_r = -30$ °C.

compared with for ordinary solid samples. However, the tensile stress and retardation could be measured precisely, and therefore determination of C_G (as a ratio of retardation to stress) and the resulting solution of the MSOR equations (for force and retardation) were performed with enough accuracy. The overall accuracy of the final value of the stress–optical coefficients and component functions was less accurate, reflecting the uncertainty of geometrical factors. The obtained components are shown in Figure 5. The MSOR separation is satisfactory. The characteristic features of the two components are similar to those for melts. One minor difference is that each component is broader than that for bulk.

Similar results were obtained at other concentrations. The results are shown in Figures 6–8. The proportionality between O' and E' is somehow less satisfactory at low concentrations, particularly at high frequencies, and therefore unreasonable results at high frequencies are omitted (for example, $\log \omega a_T > 5$ in Figure 8). Compared with the data for PS in bulk,⁴ the shapes of the component functions are broad: For example, maximum of E_G'' is not clear for f288/60. With decreasing concentration, the maximum of E_G'' becomes clear. These results may be attributed to effect of concentration fluctuation or dynamic heterogeneity. On the other hand, E_R'' around its maximum becomes broad with decreasing concentration. This result suggests that the concentration fluctuation may affect the R and G components in different ways.

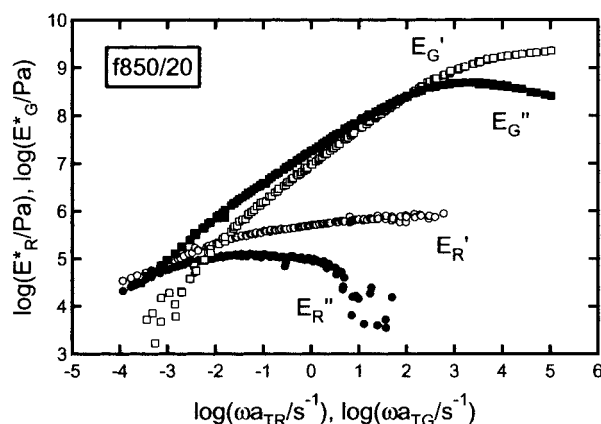


Figure 8. Component functions for f850/20 solution. $T_r = -40$ °C.

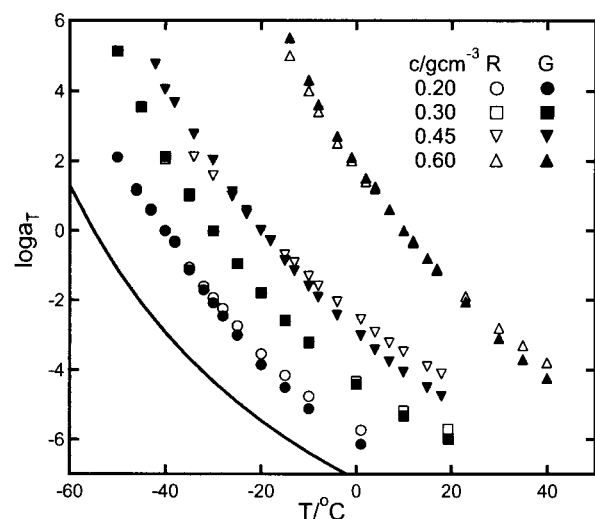


Figure 9. Temperature dependence of shift factors for R and G components.

Temperature Dependence of Component Functions. Figure 9 shows the temperature dependence of shift factors for the component functions. Shift factors for the G component show a stronger temperature dependence similarly as for in the melt. The obtained temperature dependence of the R and G components shows a good correspondence with data for the viscosity and the recoverable compliance of PS/TCP solutions, respectively,⁴ although a precise quantitative discussion is difficult because of the difference in concentration.¹³

Concentration Dependence of M_S . The Rouse segment size was calculated from the limiting modulus for the R component, $E_R'(\infty)$ with eq 4. Figure 10 displays the concentration dependence of the Rouse segment size. Also included are data for melt⁴ and data for PS/Aroclor dilute solutions.^{9,10} Here we selected data analyzed with eq 6 for samples having $M > 2 \times 10^4$ and narrow molecular weight distributions.

Before discussing the concentration dependence of M_S , we would like to comment on the effect of solvent species. Our data do not cover the dilute regime, and therefore we performed a preliminary measurement on η^* of PS/TPC solution at 1%. The data were analyzed with eq 7. Here, we substitute $\eta^*(\omega)$ of neat TCP for $\eta^*(\omega)$ in eq 7 with a correction of relaxation time. (The time scale of $\eta^*(\omega)$ was shifted so that $\tan \delta$ of neat TCP and PS/TCP solutions agreed with each other at high frequencies.) This analysis provided us $M_S \sim 5000$

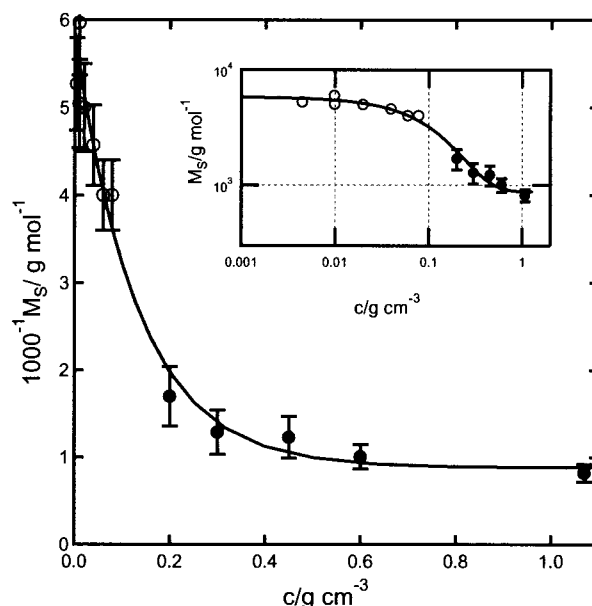


Figure 10. Concentration dependence of M_S : filled circles, present results; open circles, OFB data.¹⁰ See text for continuous lines.

although the obtained η^*_{Poly} data were limited at high frequencies. This result strongly suggests that difference of solvent is negligible as the first approximation. Thus, we ignore the difference of solvents in the following discussion.

We check the consistency between the present data and flow birefringence data for dilute solutions by fitting a simple exponential function. The result shown in Figure 10 is

$$M_S = 883 + 4960 \exp(-c/0.133) \quad (11)$$

All data lie on this fitting function within error bars although another fitting function may provide better description. We may conclude that M_S depends on concentration and characteristic concentration, c_c , is about 0.1 g cm^{-3} . The results, $c_c \sim 0.1 \text{ g cm}^{-3}$, strongly suggest that the molecular origin of concentration dependence of M_S is probably due to polymer-solvent molecular interactions. Significant molecular interactions would be screened out in the scale of Rouse segment at high concentrations.

Concentration Dependence of C_R . The stress-optical coefficient, C_R , is also a measure of segment size. As described in Introduction, C_R is proportional to the size of segment and anisotropy of repeating unit, $\Delta\alpha$.^{15,16} For the case of polymer solutions, $\Delta\alpha$ may depend on concentration due to the inductive effect. Another effect creating concentration dependence of C_R is the nematic effect. The nematic effect increases C_R , and it is significant only for melts.¹⁹

Figure 11 shows the concentration dependence of C_R and C_G . Here, C_R data are reduced at 0 °C considering $C_R \sim 1/T$. With decreasing concentration, C_G increases about 2 times of that for bulk, while C_R decreases only 20%, suggesting the size of optical segment may be almost constant. Here it may be worthwhile to note that the dependence of $\langle R_g^2 \rangle$ on M for PS in TCP in dilute regime with $10^4 < M < 10^5$ is very well described by Nb^2 , which means that the $\langle R_g^2 \rangle$ does not vary with concentration.²⁰ Therefore, it is strongly suggested that

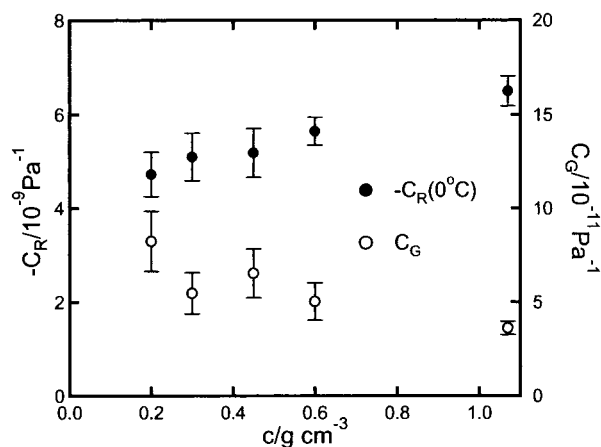


Figure 11. Concentration dependence of the stress-optical coefficients at 0 °C: filled circles, C_R ; open circles, C_G .

$\Delta\alpha$ and the size of the optical segment remain almost constant as the Kuhn segment does.

Significant variation of C_G may suggest that C_G of TCP would be larger than that of polystyrene. The TCP molecules may orient much more easily than the repeating unit of PS because they do not have any intermolecular linkage. Flow birefringence measurements of TCP solvent around the glass transition temperature are interesting. However, it is difficult for our apparatus.

Discussion

Significance of the Rouse Segment. The Rouse segment is calculated from the limiting modulus, $E_R'(\infty)$, which can be related with the orientational birefringence induced by instantaneous deformation ($\omega \rightarrow \infty$), Δn_{R0} .

$$\Delta n_{R0} = C_R E_R'(\infty) \epsilon \quad (11)$$

Here ϵ is the elongational strain. $C_R E_R'(\infty)$ represents how much the birefringence is created in the glassy zone by unit deformation, and therefore $E_R'(\infty) = \Delta n_{R0}/C_R$ has a meaning of the main chain orientation induced per unit strain. Thus, $E_R'(\infty)/c \sim 1/M_S$ represents the main chain orientation per strain, and therefore M_S would reflect mechanical rigidity of the chain. Note that at $\omega \rightarrow \infty$ responses of polymer and solvent molecules are essentially elastic. The difference in the relaxation time between polymer and solvent molecules does not affect the present discussion.

The present experimental results show that the Rouse segment size increases with decreasing concentration. This means that main chain orientation of a chain per unit strain decreases with decreasing concentration. In other words, relative rigidity of chain to the surrounding medium increases with decreasing concentration. On the other hand, the measure of optical segment size, C_R , remains constant over a studied concentration regime. These results indicate that *the segment size as orientational unit for given stress* would not vary with concentration, but *the orientation of chain for unit strain* in the glassy zone decreases with decreasing concentration.

Measurements on dilute solutions were mostly performed by using glass-forming solvents with high viscosity in order to achieve slower polymer chain dynamics. Therefore, glass-forming nature of solvent has been discussed as origin of anomalously large M_S .¹⁰ Amelar

et al. suggest that for the case of PS/Aroclor system the reorientational mobility of the Aroclor molecules is significantly retarded by the presence of the PS chains. The Aroclor molecular dimension is within a factor of 2–3 of R_g of a 50 monomer PS chain, and furthermore Aroclor is a glass-forming liquid so that its molecules may well exhibit significant intermolecular orientational correlation. Dynamic rigidity in the solvent may inhibit relative polymer/solvent motion, and therefore M_S may become larger than the intrinsic chain flexibility. However, if this is true, the *orientational unit for given stress* should be the same as M_S . Significant intermolecular orientational correlation would result in change of statistical properties of chain, and the C_R would vary as the case of the nematic effect. Thus, the above speculation contradicts the present results, indicating that intrinsic dynamic rigidity measured as segment of stress would not be varied so much by the presence of the solvent. Constancy of C_R indicates that the conformational transitions of chain occur in the scale of the intrinsic chain flexibility, and therefore chain modes (Rouse modes) in the scale of the intrinsic chain flexibility would survive.

We again address that the Rouse segment is conceptually related to the response at $\omega \rightarrow \infty$. Deformation of a mixture of solvent and polymer at $\omega \rightarrow \infty$ would be inhomogeneous in local scale. After an instantaneous deformation, the polymer chains and the solvents would change their position and orientation probably as close to as affine deformation. Deformation of chemical bonds causes large strain energy. This strain energy would be minimized by deviation from affine deformation. Compared with solvent molecules, structure units of polymer chain are connected by chemical bond, and therefore the polymer would not be deformed so freely, and probably main chain orientation would be *suppressed*. Thus, we expect that local strain distribution in solution is inhomogeneous. On the other hand, polymer melts are a single-component system, and therefore strain distribution would be homogeneous in smaller scales.

Summary

Stress and birefringence of polystyrene solutions were measured simultaneously, and data were analyzed with the modified stress optical rule. The Rouse segment size estimated from orientational birefringence increased with decreasing concentration. The Rouse segment can be related to the segment orientation produced by instantaneous deformation, and therefore the present result can be interpreted as the decrease of segment orientation for given strain with existence of solvent molecules, particularly deformation at short spatial scales. On the other hand, another measure of segment size, the stress-optical coefficient, was found to be insensitive to concentration. This means that the orientation produced by given stress remains almost constant. Constancy of the stress-optical coefficient indicates that the conformational transitions of chain in the Kuhn segment size, $M \sim 1000$, occurs, and it is suggested that dynamic properties such as the smallest Rouse mode may not be affected by the presence of solvent molecules. A possible speculation is that the Rouse segment reflects inhomogeneous deformation of polymer solution.

References and Notes

- (1) Janeschitz-Kriegl, H. *Polymer Melt Rheology and Flow Birefringence*; Springer-Verlag: Berlin, 1983.

- (2) Osaki, K.; Inoue, T. *Macromolecules* **1996**, *29*, 7622.
- (3) Inoue, T.; Onogi, T.; Osaki, K. *J. Polym. Sci., Part B: Polym. Phys.* **2000**, *38*, 954.
- (4) Inoue, T.; Okamoto, H.; Osaki, K. *Macromolecules* **1991**, *24*, 5670.
- (5) Inoue, T.; Matsui, H.; Murakami, S.; Kojiya, S.; Osaki, K. *Polymer* **1997**, *38*, 1215.
- (6) Okamoto, H.; Inoue, T.; Osaki, K. *J. Polym. Sci., Polym. Phys. Ed.* **1995**, *33*, 417.
- (7) Inoue, T.; Osaki, K. *Macromolecules* **1996**, *29*, 1595.
- (8) Massa, D. J.; Schrag, J. L.; Ferry, J. D. *Macromolecules* **1971**, *4*, 210.
- (9) Sammler, R. L.; Landry, C. J. T.; Woltman, G. R.; Schrag, J. L. *Macromolecules* **1990**, *23*, 2388.
- (10) Amelar, S.; Eastman, C. E.; Morris, R. L.; Smeltzly, M. A.; Lodge, T. P.; von Maxwell, E. D. *Macromolecules* **1991**, *24*, 3505.
- (11) Nagasaka, K.; Yoshizaki, T.; Yamakawa, H. *J. Chem. Phys.* **1989**, *90*, 5167.
- (12) White, C. C. Ph.D. Thesis, 1994.
- (13) Riande, G.; Markovits, H.; Plazek, D. J.; Raghupathi, N. *J. Polym. Sci., Polym. Symp.* **1975**, *50*, 405.
- (14) Inoue, T.; Onogi, T.; Osaki, K. *J. Polym. Sci., Polym. Phys. Ed.* **1999**, *37*, 389.
- (15) Treloar, L. R. G. *The Physics of Rubber Elasticity*; Clarendon: Oxford, 1958.
- (16) Volkenstein, M. V. *Configurational Statistics of Polymeric Chains*; Interscience: New York, 1963.
- (17) Ferry, J. D. *Viscoelastic Properties of Polymers*; Wiley: New York, 1980.
- (18) Osaki, K.; Inoue, T.; Hwang, E. J.; Okamoto, H.; Takiguchi, O. *J. Non-Cryst. Solids* **1994**, *172–174*, 838.
- (19) Doi, M.; Watanabe, H. *Macromolecules* **1991**, *24*, 740.
- (20) Lodge, T. P.; Hermann, K. C.; Landry, M. R. *Macromolecules* **1986**, *19*, 1996.

MA011037M